Fibers and Polymers 2020, Vol.21, No.12, 2915-2926
DOI 10.1007/s12221-020-1284-8

ISSN 1229-9197 (print version)
ISSN 1875-0052 (electronic version)

Crystallization and Mechanical Properties of Glass Fiber Reinforced Polypropylene Composites Molded by Rapid Heat Cycle Molding

Aimin Zhang*, Guoqun Zhao*, Jialong Chai, Junji Hou, Chunxia Yang, and Guilong Wang*

Key Laboratory for Liquid-Solid Structural Evolution and Processing of Materials (Ministry of Education), Shandong University, Jinan, Shandong 250061, China

(Received December 12, 2019; Revised March 6, 2020; Accepted March 25, 2020)

Abstract: The crystalline behavior and mechanical properties of PP/GF (glass fibers) composites molded by rapid heat cycle molding (RHCM) and conventional injection molding (CIM) were compared. SEM, DSC and XRD were utilized to study crystallization behavior of PP and PP/GF composites. Furthermore, universal testing machine was employed to investigate the mechanical properties. Results proved that higher degree of crystallinity and larger crystal size can be obtained in RHCM in comparison to CIM. GF can induce more crystal nuclei and then reduce the crystal size due to shear stress which is generated in polymer matrix around fibers. Nucleating agent (NA) has a positive effect on refine grains. The average crystal diameter of PP/NA/30 %GF is about 1.7 μm which is one-tenth of PP/30 %GF (14 μm) in RHCM. XRD tests illustrated that α-form crystal is the main crystal type for PP and PP/GF composites in RHCM and CIM. However, there is a little β-form crystal in RHCM for PP/GF composites without NA. NA accelerates the formation of α-form crystal and restrains the emergence of β-form crystal. The plastic parts obtained in RHCM exhibited higher strength and modulus compared with that obtained in CIM for both tensile and flexural tests.

Keywords: Crystallization, Mechanical properties, Polypropylene, Rapid heat cycle molding, Nucleating agent

Introduction

Polymer and polymer composites with lower densities than metal and ceramic materials have been widely used in almost all facets of modern economy. Injection molding method is an important approach to fabricate large-sized and shape-complicated polymer products. However, there are many appearance defects including weld lines, flow marks, crazing defects and floating fibers in conventional injection molding (CIM) products [1]. This is mainly because the mold temperature is kept at a constant value lower than the ejection temperature of polymer parts [2]. The rather cold mold makes polymer melt frozen in advance during filling stage. Polymer melt cannot duplicate the mold surface precisely and thus many surface defects may be formed.

Rapid heat cycle molding (RHCM) technology is an innovative approach to address the surface problem once and for all. A dynamic mold temperature strategy is introduced into RHCM process. The mold cavity is rapidly heated up to a relatively high temperature before filling stage. During filling and packing stage, the mold should be always kept at high temperature in order to improve the flow ability of the polymer melt. At the end of packing stage, the mold cavity is cooled down quickly so as to freeze the polymer melt for demolding. And then the mold will be heated again for the next injection cycle. Since the mold cavity temperature is always kept at a high level during filling and packing stage, the flow ability of polymer melt is significantly improved and the premature freezing of polymer melt during filling stage is avoided. Accordingly, polymer products with excellent appearance can be obtained in RHCM process.

The rapid heating and cooling method of mold as well as structure and properties of plastic parts are two critical issues in RHCM process. The rapid heating and cooling methods have been of great interest to researchers for recent years [3-9]. And the heating and cooling efficiency together with the devices' flexibility have been greatly enhanced and the mold temperature control scheme has been mature. The effect of processing parameters on surface properties have gained much attention during the past ten years. It is demonstrated that RHCM process can greatly increase the gloss of plastic parts and eliminate surface defects [10-13].

Since the greatest advantage of RHCM technology is perfect surface quality of plastic parts, the structural evolution of polymer in RHCM process has often been ignored. Nevertheless, the structure of polymer chains is one of the most important factors which affects the mechanical, photoelectrical properties and heat transfer performance [14-16]. Furthermore, crystallization is the main structural transformation in injection molding process for semi-crystalline polymer. The temperature and shear rate of polymer melt in RHCM process is quite different from that in CIM process since the mold temperature is dynamic in RHCM while it is almost static in CIM. Thus the orientation and crystallization of polymer chains exhibit unique characteristics in RHCM [17]. The crystallization morphology of polymer part will change greatly with the mold temperature in RHCM process. Thus the crystallization behavior of semi-crystalline polymers in RHCM process is also a challenging

*Corresponding author: zhangam@sdu.edu.cn
*Corresponding author: zhaogq@sdu.edu.cn
*Corresponding author: guilong@sdu.edu.cn

and significant issue.

Polypropylene (PP) is an important semi-crystalline polymer with many merits, such as low cost, high heat distortion temperature, excellent chemical resistance and good dimension stability [18]. It is widely used in various industrial fields including packaging, automobiles, insulation and electronics. Glass fibers (GF) are usually incorporated into PP polymer to enhance the comprehensive properties of PP [19,20]. PP/GF composites have drawn intensive attention owing to their excellent mechanical properties and dimensional stability. Molecular chains of PP are easy to arranged orderly and the crystallinity is usually high. It is a polymorphic material that has four modifications, the monoclinic α-phase, trigonal β-phase, orthorhombic γ-phase, and smectic mesophase. And the crystallization morphology could exhibit different forms as the processing parameters changed [21]. The crystallization behavior of PP in injection molding process have been investigated in the past decade [22-25]. Some studies have demonstrated that injection molding parameters especially the molding temperature and cooling rate play great important roles on crystal structure of polymer products in CIM process. Suplicz [23] found the crystallinity is decreased when the cooling rate of mold is too high. Salah [24] found that the crystallinity of polymer gradually increases from the external surface layer to the core of plastic parts due to temperature and pressure variation in mold cavity in CIM process. However, the crystallization behavior of crystalline polymers in RHCM process has not got much attention.

In this paper, we focus to the crystallization and mechanical properties of GF reinforced PP composites molded by RHCM. It is of great significance to understand the crystallization behavior of PP/GF in RHCM. We prepared PP/GF composites with different GF content in a co-rotating twin screw extruder. As we all know, nucleating agent and injection process are the dominant factors affecting crystallization behavior of plastic parts. In order to compare the mechanism of nucleating agent in RHCM and CIM process, MNA-108 nucleating agent (NA) usually used for PP is introduced to change the crystal structure of PP and PP/GF in RHCM and CIM process. Herein, PP, PP/NA, PP/GF, PP/NA/GF are prepared by melt blending. Both CIM and RHCM processes are used to mold the plastic parts. Scanning electron microscopy (SEM) was employed to demonstrate the crystal shapes and sizes of plastic parts in RHCM and CIM. Differential scanning calorimeter (DSC) was used to analyze the non-isothermal crystallization behavior of PP and PP/GF composites. X-ray diffraction (XRD) was used to confirm the crystal form and degree of crystallinity. The crystal form and degree of crystallinity of surface and core of plastic parts in thickness direction were compared. Finally, the mechanical properties of all the composites were evaluated by using universal testing machine. The tensile strength, tensile modulus, elongation at break, flexural strength and flexural modulus of PP, PP/NA, PP/GF, PP/NA/GF were calculated.

Experimental

Materials

The commercially available PP, PPH-M17 (V30G), was purchased from Sinopec Zhanjiang Dongxing Petrochemical Co., Ltd. in a pellet form. PP has a melt flow index of 18.4 g/10 min (230 °C/2.16 kg) and anisotacticity of 96.8 %. WNA-108 is a kind of substituted aryl carboxylates aluminum salts α-nucleating agent which is supplied by Guangdong Winner new material Technology Co., Ltd. And the glass fibers (GF) with a length of 3 mm were provided by Zhejiang Tong xiang Ju shi Group.

Materials Blending

In order to investigate the crystallization and mechanical properties of PP/GF plastic parts molded by RHCM process, PP/GF and PP/NA/GF with different GF content were prepared in a co-rotating twin screw extruder with a screw diameter of 21 mm and length to diameter ratio of 36. Before blending in co-rotating twin screw extruder, all of the materials were put into a vacuum drying oven at 70 °C for 10 h to remove moisture. The materials with different component according to Table 1 were premixing in a container. And then they were blended in a co-rotating twin screw extruder. The temperature profile of 180-190-200-210-220-210-200 °C of extruder was set from the hopper to the die. The feed rate was kept at 3.6 kg/h and the screw speed was set at 120 rpm. The extrudate from die was shaped into cylindrical strands, led into a water bath and finally pelletized by a cutting chamber. All the pellets were further dried at 70 °C for 10 h to remove the moisture before characterization and injection molding. PP was also extruded from the co-rotating twin screw extruder to obtain the same thermal and shear history.

Injection Molding

An electric heating RHCM system was developed in our laboratory. Two heating rods with the power of 15 w/cm^2 were used for each sample in order to heat the mold quickly. Cooling water pipes were arranged vertical to heating rods. Six specimens according to ASTM standard specifications were molded in each injection cycle. The RHCM system was built on the platform of MA3200 injection molding machine. The diagram of RHCM process is showed in Figure 1. Before filling stage the mold temperature control system asked the heating rods to work and prepare for filling. After filling stage, cooling water from the cooling tower was pumped into the cooling pipes. Then the condensed air made by condenser entered into the cooling pipes of the mold. The water in the cooling pipes was blown out and another injection cycle began to start.

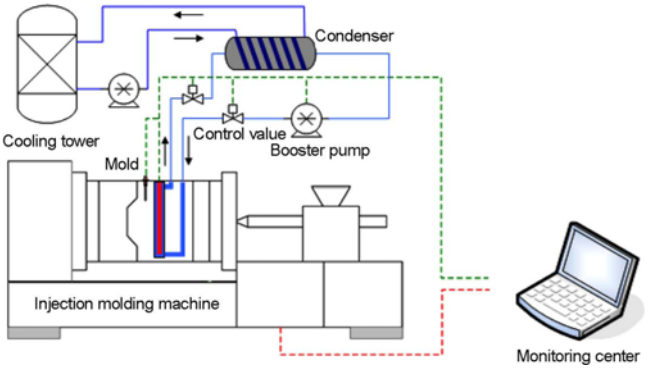

Figure 1. Scheme of RHCM platform.

Table 1. Component of composites and molding methods

Code	PP	Glass fiber (phr)	NA (phr)	Molding method
1	100	0	0	CIM
2	100	0	0	RHCM
3	100	0	0.5	CIM
4	100	0	0.5	RHCM
5	100	10	0	CIM
6	100	10	0	RHCM
7	100	30	0	CIM
8	100	30	0	RHCM
9	100	10	0.5	CIM
10	100	10	0.5	RHCM
11	100	30	0.5	CIM
12	100	30	0.5	RHCM

CIM: conventional injection molding and RHCM: rapid heat cycle molding.

Then plastic samples were molded using RHCM process or CIM process. The mold temperature was kept at 100 ^{o}C during filling stage in RHCM process while the mold temperature is always kept at 40 ^{o}C in CIM process. Other injection parameters such as melt temperature, injection time, packing pressure and packing time were all kept constant.

Characterization

SEM Test

A JEOL 6610-LV scanning electron microscopy (SEM) was used to observe the morphology of composites. To characterize the crystal morphology, the samples were firstly cryo-fractured in liquid nitrogen to get the vertical sections as illustrated in Figure 2(surface A). Then the cryo-fractured surfaces were etched for 20 hours to remove amorphous regions by the permanganic etching technique [26]. The etching reagent was composed of a 1 % w/v solution

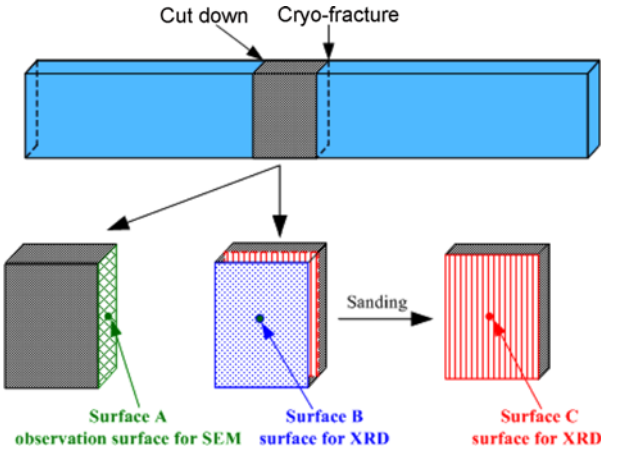

Figure 2. Preparation of samples for SEM and XRD characterization.

potassium permanganate ($KMnO_4$) in an acid mixture with 10 parts concentrated sulfuric acid (H_2SO_4), 4 parts concentrated phosphoric acid (H_3PO_4) and 1 part distilled water. Then, the etched surface was coated with a thin layer of platinum prior to SEM observation.

DSC Test

A Q2000 differential scanning calorimeter (DSC), TA Instruments, USA, was used to analyze the non-isothermal crystallization behavior of PP and PP/GF composites. The sample was heated from 25 °C to 200 °C at a heating rate of 10 °C/min and then isothermally treated at 200 °C for 5 min to remove its thermal history. Subsequently, the sample was cooled to 25 °C at a cooling rate of 10 °C/min to acquire the exothermic peak resulted from crystal formation. Then, the sample was once again heated to 200 °C at a heating rate of 10 °C/min to attain the endothermic peak caused by crystal melting. Finally, the sample was cooled to 25 °C at a cooling rate of 25 °C/min to complete the test. The cylindrical particles from the extruder were used in DSC test.

The DSC test was repeated three times for each sample, and the average values were calculated. To estimate the effect of NA and glass fibers on the crystallization behavior of PP, the DSC thermograms were analyzed using the TA universal software. The degree of crystallinity of PP was calculated using the following equation:

$$x_c = \frac{\Delta H_c}{\Delta H_c^{o} \times \omega} \times 100 \quad (1)$$

where ΔH_c is the measured crystallization enthalpy, ΔH_c^{o} is the 100 % crystallization enthalpy, and ω is the weight fraction of PP in the composite. The value of ΔH_c^{o} was assumed to be 209 J/g for PP [27].

XRD Test

XRD was carried out on a DMAX-2500PC X-ray diffractometer (Rigaku Co., Japan) with a Cu K_α source and an average wavelength of 1.542 Å. The experiment was conducted at 45 kV and 35 mA under ambient temperature.

And the scan range was between 3 ° and 50 ° with a scan rate of 2 °/min. In order to investigate the crystal structure of injection plastic parts, Surface B of plastic parts on the side of moving mold half as shown in Figure 2 was selected for XRD measurements. Then samples were sanding by sand papers to half the thickness. The new sanded surface (surface C shown in Figure 2) was also be measured by XRD to investigate the crystal structure in core region. Equation (2) was used to calculate the degree of crystallinity [28].

$$\chi_c = \frac{A_c}{A_c + A_a} \quad (2)$$

where A_c and A_a were the total crystalline and amorphous area obtained from XRD patterns, respectively.

Mechanical Test

Tensile tests were carried out on a CMT 4204 20KN universal testing machine (maximum load: 20 KN) at ambient temperature according to ASTM D638 [29]. The crosshead speed was kept at 5 mm/min. And flexural tests were also carried out on a CMT 4204 20KN universal testing machine (maximum load: 20KN) at ambient temperature according to ASTM D790 [30]. The crosshead speed was kept at 2.0 mm/min and the support span is 16 times specimen depth. At least five samples were tested for each property and the average values were calculated.

Results and Discussion

Crystallization Behavior

Comparison between RHCM and CIM Methods

Crystallization is the chief form of structural evolution of polymer melt in injection processing. Furthermore, crystallization morphology of polymer matrix has significant influence on final properties of polymer plastic parts. Thus controlling crystallization behavior of polymer material becomes an important and key approach to modify final properties of plastic parts. As we all know, the polymer matrix's crystallization is closely associated with its thermal history. However, the rapid heating and cooling of mold cavity in RHCM process make polymer melt's thermal history quite different from CIM process. Herein, we compared the crystallization of PP/GF composites in RHCM and CIM process.

Figure 3 illustrates the crystallization morphology of polymer matrix away from fibers in RHCM and CIM process. The crystals are marked by red circles as shown in Figure 3. Spherulites can be found in plastics parts molded by both RHCM and CIM process, but the crystal size is different. In RHCM plastic parts, the average diameter of crystal size is about 14 μm while it is about 8 μm in CIM plastic parts. This means that the spherulite can grow more perfect and bigger in RHCM process compared with CIM process. Different mold temperatures between RHCM and CIM process may be responsible for it. Mold temperature directly influences polymer temperature, and further influence the crystallization behavior of polymer.

Figure 4 shows the schematic illustration of mold temperature in RHCM and CIM process and the relationship between crystallization speed and polymer temperature. The crystallization process mainly consists of two stages, namely, nucleation and crystal growth which are driven by thermodynamic properties as well as chemical properties.

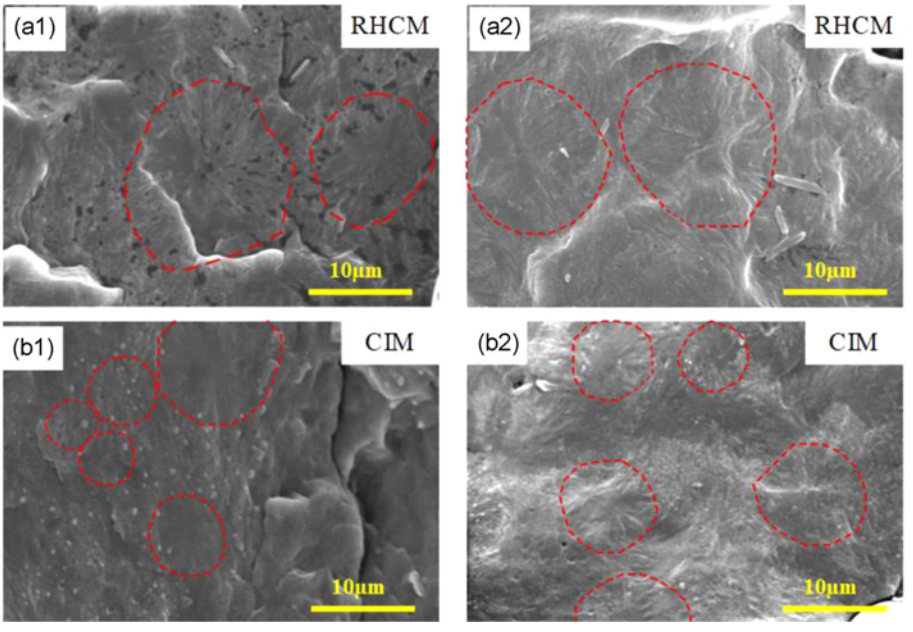

Figure 3. Crystallization morphology of polymer matrix (PP/30 %GF) away from fibers in RHCM and CIM process; (a1) and (a2) samples molded in RHCM process and (b1) and (b2) samples molded in CIM process.

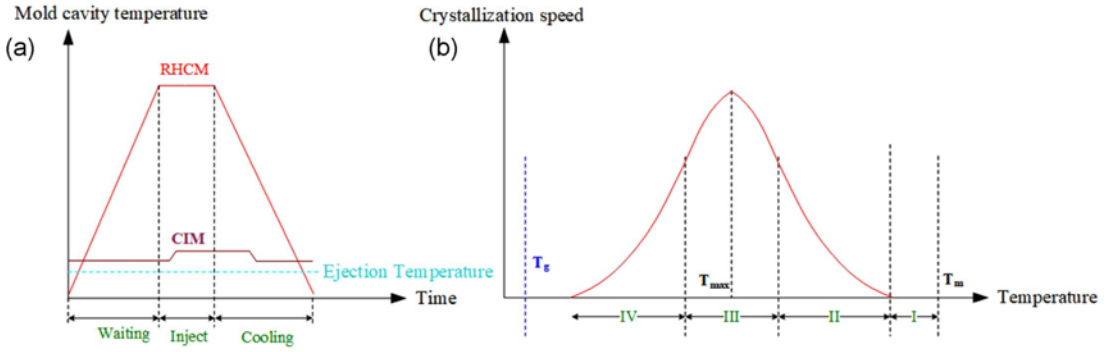

Figure 4. Schematic illustration of mold temperature in injection process and the relationship between crystallization speed and temperature of polymer melt.

Crystallization occurs between T_g (glass transition temperature) and T_m (melting temperature) of polymer melt. In a certain temperature range below T_m (Zone I in Figure 4(b)) the nucleation of polymer matrix is difficult and the crystallization speed is zero due to very low nucleation driving force. Crystallization speed increases rapidly with the decrease of temperature as shown in Figure 4(b). However, when the temperature is decreased to zone II crystal growth rate is accelerated and crystallization was promoted. The crystallization speed continues to increase with the decrease of temperature. And the highest crystallization speed can be found in zone III in which the nucleation rate and crystal growth rate are both high. The nucleation of polymer matrix is easier during higher degree of under cooling with further decrease of temperature. So the crystallization speed is mainly controlled by nucleation process in zone IV. But it is hard for crystal growth during lower temperature in zone IV. That is why the crystallization speed becomes to decrease with further decrease of temperature.

In CIM process, the polymer melt is quickly cooled as soon as it contacts the mold cavity since the mold temperature is relatively low as shown in Figure 4(a). The high cooling rate of melt is beneficial to nucleation of spherulite but unfavorable for crystal growth. There is not enough time for crystals to grow bigger under low temperature. However, in RHCM process the mold temperature is high and the pre-frozen layer is avoided in filling stage. The polymer melt has a long residence time in zone III and IV. The crystallization speed is high and the crystal growth is going well in these temperature zones. Therefore, the crystal size is bigger in RHCM process.

Figure 5 demonstrated XRD patterns of surfaces for PP/30 %GF and PP/NA/30 %GF composites in RHCM and CIM process. Surface B as shown in Figure 2 was chosen to characterize by XRD test. It is noticed that the diffraction patterns show the strongest diffraction peaks at 2θ of 13.8°, 16.8°, 18.3°, 21° and 21.8° which represent (110), (040), (130), (131), (041) crystalline planes of α-form crystal of PP. These results exhibit that both PP/30 %GF or PP/NA/30 %GF composites in RHCM and CIM have a proper orientation of polymer chains and polymer matrix has the α-monoclinic crystal structure. The detailed investigation of respective peaks for PP/30 %GF composites makes it clear that the diffraction peak at 2θ of 16.8° is the strongest crystal peak. Furthermore, it is demonstrated the crystal peak at 2θ of 16.8° is higher in RHCM than that in CIM whether for PP/30 %GF or PP/NA/30 %GF composites. These results exhibit that polymer chains can be better arranged periodically and the degree of crystallinity is higher in RHCM compared in CIM. The degree of crystallinity of PP/30 %GF or PP/NA/30 %GF composites is calculated as shown in Table 2 according to equation (2). It is obvious that the degree of

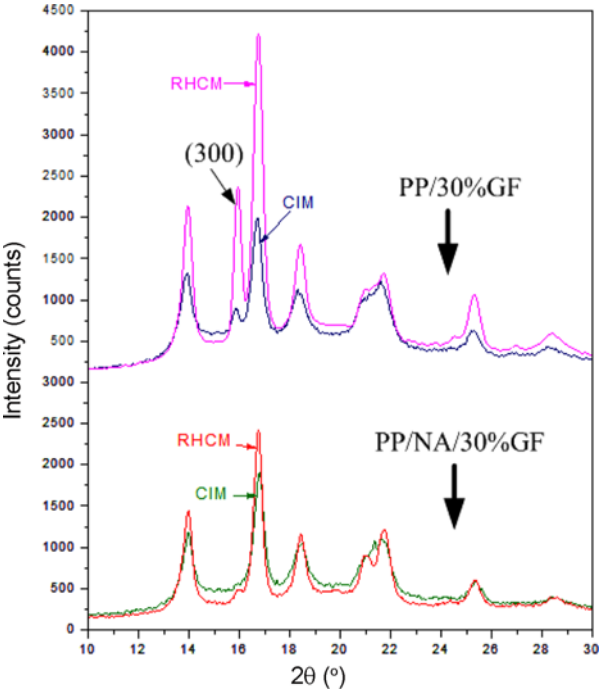

Figure 5. XRD patterns of surfaces for PP/30 %GF or PP/NA/30 %GF composites in RHCM and CIM process.

Table 2. Degree of crystallinity χ_c of PP composites calculated from XRD

	PP/ 30 %GF CIM	PP/ 30 %GF RHCM	PP/NA/ 30 %GF CIM	PP/NA/ 30 %GF RHCM
χ_c (%)	41	59	56	82

crystallinity of both PP/30 %GF and PP/NA/30 %GF in RHCM is higher than that in CIM. As expected the degree of crystallinity of PP/NA/GF is much higher than PP/GF despite the molding method.

The analysis by using Jade software indicates that the full width at half maximum (FWHM) corresponding to characteristic peak of (040) crystal plane for XRD patterns is 0.393 (PP/30 %GF in CIM), 0.278 (PP/30 %GF in RHCM), 0.434 (PP/NA/30 %GF in CIM) and 0.390 (PP/NA/30 %GF in RHCM), respectively. Generally, the higher the FWHM is, the smaller the crystal is. The crystal size is larger in RHCM than in CIM for both PP/30 %GF and PP/NA/30 %GF according to HWHM from XRD patterns. This is consistent with SEM micrographs. It is proved again that the growth of crystal is going well in RHCM compared with CIM. RHCM is a grateful molding method which is beneficial for the crystallization of PP and PP/GF composites.

However, it can also be found that a distinct diffraction peak at 2θ of 16° has appeared for PP/30 %GF composites in RHCM while the diffraction peak is weak in CIM. It is generally known that the important characteristic peak for the β phase of PP is usually found at diffraction angle around 2θ of 16°. It is inferred that a certain amount of β-form crystal is formed in RHCM for PP/30 %GF composites while only tiny amount of β-form crystal is formed in CIM. RHCM process is beneficial for the formation of β-form crystal.

The is a kind of hexagonal crystal usually formed under special conditions, such as special temperature gradient, shear orientation and using β nucleating agent. In RHCM, the mold is heated up to high temperature during filling stage and rapidly cooled down to the ejection temperature in one injection circle. The skin polymer keeps at high temperature during the whole filling stage and then it is cooled by cooling water rapidly. β-form crystal crystalline time in range of appropriate temperature is adequate in RHCM process. The special temperature history of polymer melts benefits formation of β-form crystal [31]. However, in CIM, the skin polymer was frozen as soon as it contacts to the mold, and the heat history of polymer melt—Short residence time of elevated temperature and high cooling rate—is not beneficial for the formation of β-form crystal. Thus the diffraction peak at 2θ of 16° in RHCM is higher than in CIM for PP/30 %GF.

Unfortunately, there is no β-form crystal for PP/NA/30 %GF composites whether in RHCM or CIM process. This may be attributed to the nucleating agent (WNA-108) which is a kind of α-nucleating agent. The nucleating agent absorbs helical PP chains and restricts the movement of PP chains [32]. Thus the helical structure of PP chains is fixed and α-form crystal of PP is formed. The nucleating agent accelerates the formation of α-form crystal and restrains the emergence of β-form crystal.

Comparison between Skin and Core

The temperature and shear rate are quite different at skin and core of plastic parts in injection process. In order to investigated the crystallization of skin and core of plastic parts in RHCM and CIM, we studied surface B (skin) and surface C (core) shown in Figure 2 by XRD tests. Figure 6 demonstrated the XRD patterns of skin and core of PP/30 %GF plastic parts in RHCM and CIM process. The main diffraction peaks of skin polymer are stronger in comparison with core polymer in RHCM while it is opposites in CIM process.

The schematic diagram of cooling process of polymer melt in RHCM and CIM is given in Figure 7. In RHCM process, the skin and core polymer melt is cooled slowly in filling stage. As discussed before, crystallization mainly occurs in the temperature range of T_g and T_m of polymer melt and the T_{max} (maximum crystallization temperature) is

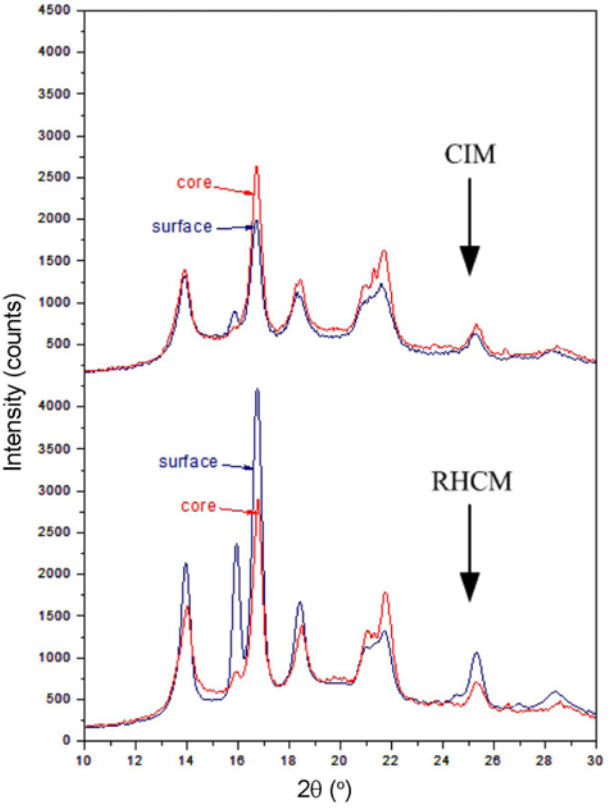

Figure 6. XRD patterns of surface and core for PP/30 %GF composites in RHCM and CIM process; (a) RHCM process and (b) CIM process.

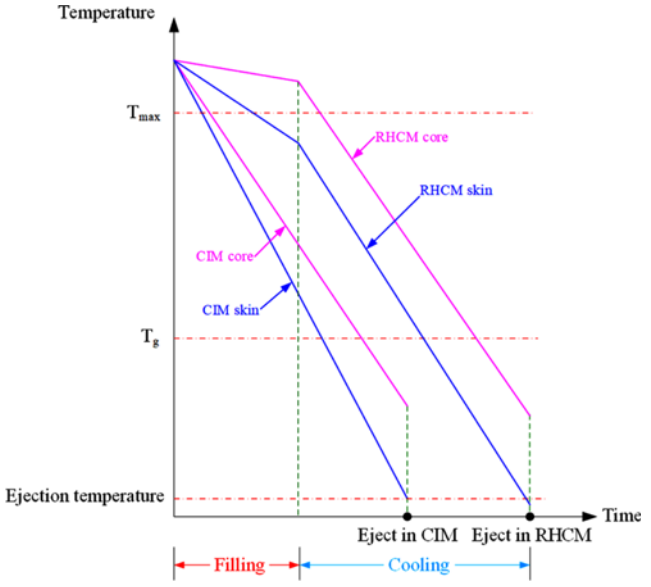

Figure 7. Schematic diagram of cooling rate of polymer melt in RHCM and CIM process.

about equal to T_m multiplied by 0.8-0.85. In RHCM process, the temperature of skin polymer melt approaches the T_{max} earlier and it can stay in the temperature range of T_g to T_{max} for a long time. However, the temperature of core polymer melt is higher than the skin. Too high temperature will decrease the crystallization rate. Moreover, the temperature of core polymer melt approaches the T_{max} later and then rapidly cooled down to the ejection temperature. So the degree of crystallinity is lower in core polymer compared with skin polymer melt in RHCM.

However, the skin polymer melt is frozen as soon as it contacts the mold cavity since the mold temperature is away below T_g of polymer matrix in CIM. Rapid cooling rate make the polymer chains cannot arrange periodically. So the skin polymer melt cannot crystallization well. The moderate cooling rate promotes crystallization of core polymer melt in CIM. Therefore, the degree of crystallinity is higher in core polymer compared with skin polymer melt in CIM.

Effect of Glass Fibers

In order to investigate the effect of glass fibers on crystallization, we compared the crystal morphology of polymer matrix around and away from glass fibers in RHCM process. Figure 8 demonstrated the crystallization morphology of polymer matrix (PP/30 %GF) around fibers in RHCM process. Figure 8(a1) illustrates a pit formed by fiber shedding and Figure 8(b1) shows a fiber embedded in the polymer matrix. Spherulites can also be found around fibers similar to Figure 3(a1) and (a2). The average crystal diameter is about 7 μm calculated from the magnification of blue box. The crystal size of polymer matrix around fiber (7 μm) is half of that away from fiber (14 μm). Due to the difference of thermal expansion coefficients between PP and glass fibers, shear stress is produced at the interface in

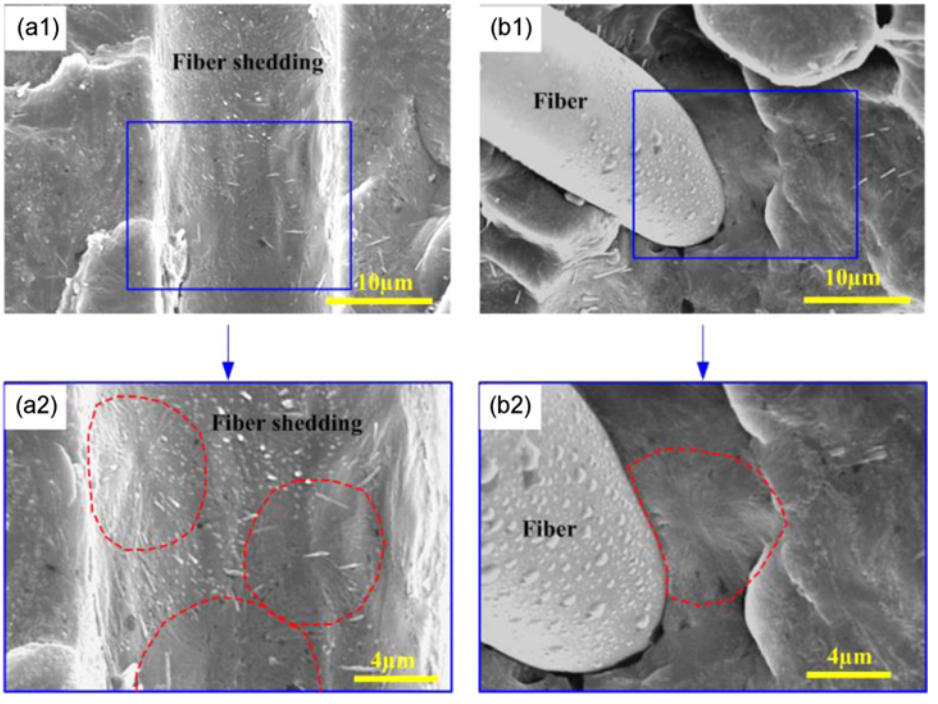

Figure 8. Crystallization morphology of polymer matrix (PP/30 %GF) around fibers in RHCM process; (a1) fiber shedding from matrix, (b1) fiber embedded in the matrix, (a2) further high magnification of part (a1), and (b2) further high magnification of part (b1).

polymer matrix. PP molecules around fibers bear shear stresses which will induce orientation of polymer molecules. Fortunately, orientation of polymer molecules is conductive to the formation of short-range ordered structure which will finally grow to the nuclei. In other words, the shear stress at the interface can induce more crystal nuclei and accelerate crystallization speed [33]. Therefore, the crystal size of polymer matrix around fibers is much smaller than that of polymer matrix away from fibers. Fibers have a good ability to promote the crystallization of PP in RHCM process.

In order to prove the above conclusion, DSC analysis was conducted. Figure 9(a) shows the DSC thermograms of pure PP, PP/NA and PP/30 %GF composites at a cooling rate of 10 °C/min. It can be found that both the peak and onset temperatures of crystallization increase significantly by adding glass fibers. It clearly demonstrates that glass fibers are good heterogeneous nucleating agent, and can accelerate the nucleation rate of PP matrix. This is consistent with SEM results in the previous session which shows that the addition of glass fibers promotes the crystallization of PP. According to equation (1), pure PP has a degree of crystallinity of 53.5 %, while the PP/30 %GF showed a degree of crystallinity of 47.0 %. It was inferred that glass fibers can only increase the nucleation speed, but not promote the crystal growth. And hence, the degree of crystallinity of PP is deduced. This phenomenon has also been reported by Wang [34].

Effect of Nucleating Agents

Nucleation is the first and critical step in crystallization. Incorporating nucleating agent into polymer has proven to be an effective method of accelerating crystallization and refine crystals for PP polymers. In order to clarify the nucleation effect of WNA-108 (α-nucleating agent) in both RHCM and CIM process Figure 3 and Figure 10 were compared in this session. Figure 3 and 10 illustrates the crystallization morphology of polymer matrix (PP/30 %GF and PP/NA/30 %GF) away from fibers in RHCM and CIM process. The morphology of PP/30 %GF exhibits spherulites in both CIM and RHCM process although the crystal size is different. However, the morphology of PP/NA/30 %GF exhibits spherulites in RHCM process but lamellae in CIM process with 0.5 wt% NA as shown in Figure 10. Nucleating agent plays the role of heterogenous nuclei and it can induce more crystal nuclei rapidly. The nuclei can be seen in the core of spherulites in Figure 10(a1) and (a2). The higher nucleation rate is, the smaller the crystal size is. Accordingly, the average crystal diameter of PP/NA/30 %GF in RHCM is about 1.7 μm which is one-tenth of PP/30 %GF (14 μm) in RHCM. This means WNA-108 can refine crystal of PP/GF in RHCM process. However, spherulites cannot be observed in Figure 10(b1) and (b2). Some lamellae marked by orange ellipse can be observed. In CIM the temperature of polymer melt is low and the activity of polymer chains is poor. Crystals cannot grow up to spherulites although there are many nucleation nuclei induced by nucleating agent. There are only some lamellae formed in CIM parts. In other words, more perfect spherulites are formed in RHCM process with 0.5 % NA compared with CIM process.

DSC thermograms of PP and PP/NA in Figure 9 demonstrated the effect of NA clearly. Similar with glass fibers, both the peak and onset temperatures of crystallization increase significantly by nucleating agent. Obviously, nucleating agent can effectively promote nucleation. However, PP/NA showed a degree of crystallinity of 54.8 % which is higher than pure PP. It is inferred that nucleating agent not only promotes nucleation but also has no adverse effect on grain growth. This is different from glass fibers.

Mechanical Properties

The mechanical properties of plastic parts are closely related to the condensed structure of polymer chains. This means the crystallization of polymer has an important

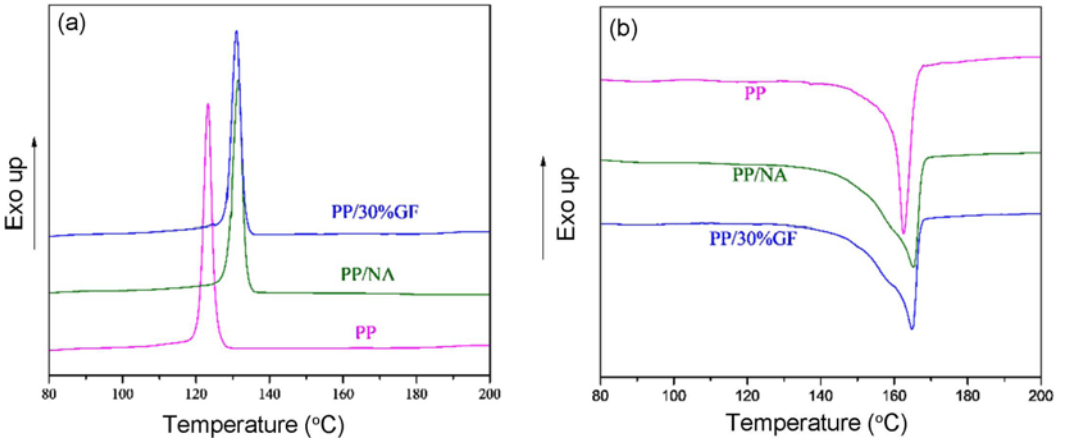

Figure 9. DSC thermograms of pure PP, PP/NA and PP/30 %GF; (a) non-isothermal crystallization at a cooling rate of 10 °C/min and (b) crystal melting process at a heating rate of 10 °C/min.

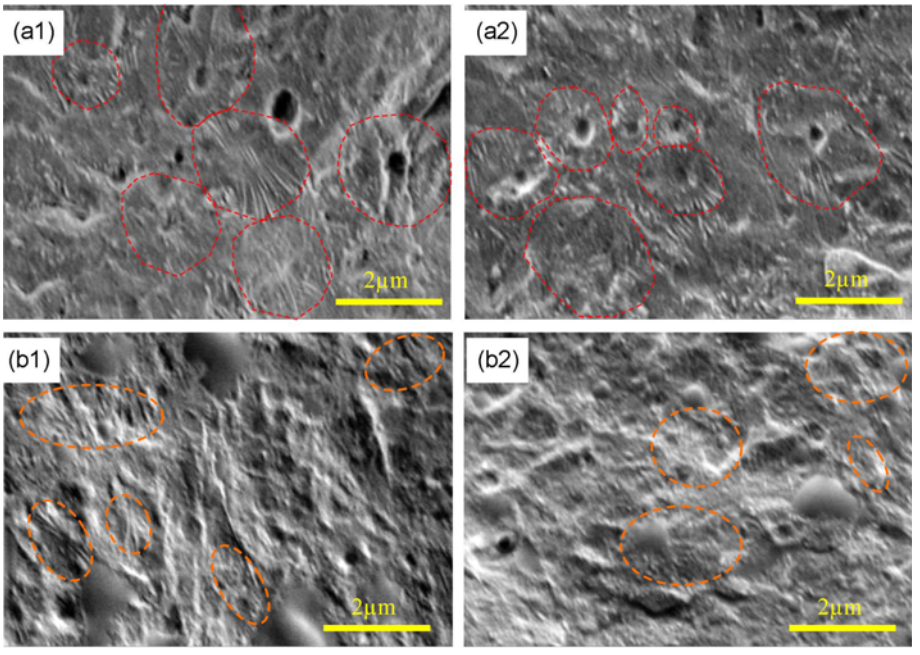

Figure 10. Crystallization morphology of polymer matrix (PP/NA/30 %GF) away from fibers in RHCM and CIM process; (a1) and (a2) samples molded in RHCM process and (b1) and (b2) samples molded in CIM process.

influence on the mechanical properties of injection plastic parts. In order to investigate the mechanical properties of PP and PP/GF composites in RHCM and CIM, tensile and flexural tests were conducted.

Figure 11 gives the mechanical properties of plastic parts with different GF contents and molding methods from tensile test. Generally, both tensile strength and modulus of RHCM plastic parts are higher compared with CIM plastic parts despite the content of GF and NA. This is mainly attributed to the higher degree of crystallinity and crystal size in RHCM plastic parts as discussed in the previous session. With the increase of degree of crystallinity of polymers, the polymer chains are arranged tightly and orderly, the porosity is reduced, and the intermolecular interaction force among polymer chains is increased. This makes the chain segments movement difficult and the tensile strength of plastic parts is improved accordingly.

The elongation at break is fundamentally related to the flexibility of polymer chains, which is related to the polymer molecular weight, condensed structure and phase structure of polymers. In this study, the flexibility of polymer chains is closely related to the crystallization of PP. Crystallization decreases the content of amorphous phase and reduces the flexibility of polymer chains. Then the activity of polymer chains is hindered and the elongation of polymer chains becomes smaller before fracture. Therefore, the elongation at break of plastic parts with the same formula in RHCM is smaller than in CIM process as shown in Figure 10. Similar phenomenon is found in ABS/GF composites studied by our team although the reasons are not exactly the same.

In order to investigate the effect of NA, PP/30 %GF composites are taken as an example. Figure 11(a) demonstrated the tensile stress-strain curves of plastic parts in RHCM and CIM process and the corresponding mechanical data are abstracted in Figure 10(b)-(d). An increase in tensile strength or modulus is expected with the adding of NA although the elongation at break is noted to decrease. The crystal size is reduced and degree of crystallinity is increased with NA which is proved by SEM microphotography and XRD test. As we all know, grain refinement is an effective way to improve the strength of materials. Thus the strength and modulus are both increased greatly by adding NA into PP/30 %GF composites despite RHCM and CIM process. However, the higher degree of crystallinity and smaller crystal size caused polymer chains difficult to stretch in tensile test. Thus the elongation at break of PP/GF composites is reduced by adding NA.

Figure 12 gives the mechanical properties of plastic parts with different GF contents and molding methods from flexural test. The effect of morphology on the flexural properties is similar to tensile properties. The flexural strength of PP, PP/10 %GF, PP/30 %GF with or without NA in RHCM is higher than in CIM due to higher degree of crystallinity in RHCM comparing with CIM. In addition, flexural strength of PP, PP/10 %GF, PP/30 %GF filled with NA increases by 3.78 %, 3.33 %, 7.52 %, respectively, comparing with unfilled PP, PP/10 %GF, PP/30 %GF in RHCM process. Meanwhile, flexural strength of PP, PP/

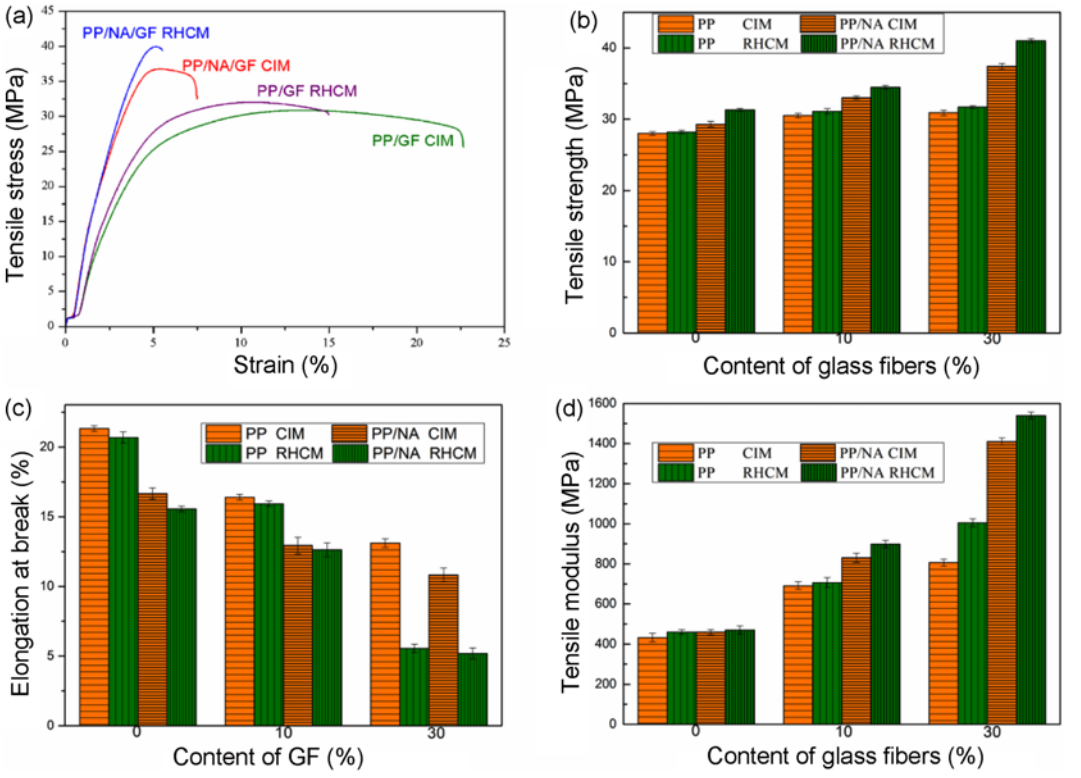

Figure 11. Mechanical properties of plastic parts with different GF contents and molding methods from tensile test; (a) tensile stress-strain curves of plastic parts with 30 %GF molded in RHCM and CIM process, (b) tensile strength, (c) elongation at break, and (d) tensile modulus.

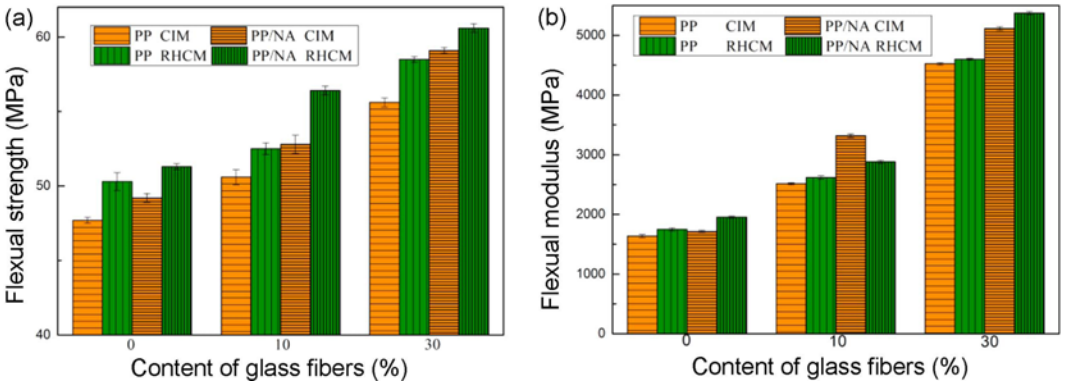

Figure 12. Mechanical properties of plastic parts with different GF contents and molding methods from flexual test; (a) flexual strength and (b) flexual modulus.

10 %GF, PP/30 %GF filled with NA increases by 3.14 %, 4.35 %, 4.23 %, respectively, comparing with unfilled PP, PP/10 %GF, PP/30 %GF in CIM process. Similar with tensile tests, flexural properties are closely related to the crystallization behavior of polymer matrix. And higher degree of crystallinity is the principle reason for better flexural properties of RHCM injection parts. In addition, the effect of NA on flexural strength is consistent with that on tensile strength. However, the variation trend of flexural modulus is similar with flexural strength in RHCM and CIM process as shown in Figure 12(b).

Conclusion

In summary, we reported two injection molding method (RHCM and CIM) to produce PP and PP/GF plastic parts. We chose WNA-108 as nucleating agent to modify the crystallization morphology of PP polymer in both RHCM

and CIM process. SEM tests showed that spherulite was the mainly crystal form in injection process and the crystal could grow more perfect and bigger in RHCM process comparing with CIM process. Otherwise, the crystal size of polymer matrix around fibers was much smaller than that of polymer matrix away from fibers since GF played an important role in promoting nucleation but restrained crystal growth. Yet, NA not only promoted nucleation but also had no adverse effect on crystal growth. The crystal size was greatly reduced with NA in RHCM process. However, there were only some lamellae formed in CIM process.

XRD tests also demonstrated the degree of crystallinity in RHCM was higher than that in CIM for the same materials. Besides, it was illustrated that α-form crystal was the main crystal type for PP and PP/GF composites in both RHCM and CIM process. However, there was a little β-form crystal in RHCM process for PP/GF composites without NA. Just because NA accelerated the formation of α-form crystal and restrained the emergence of β-form crystal, there was no β-form crystal for PP/NA/30 %GF composites whether in RHCM or CIM process.

Both tensile strength and modulus of RHCM plastic parts were higher compared with CIM plastic parts despite the content of GF and NA. An increase in tensile strength or modulus was expected by adding NA into polymers due to the higher degree of crystallinity and smaller crystal size. The variation trend of mechanical properties in flexural tests was similar with that in tensile tests for both RHCM and CIM process.

Acknowledgements

This project was financially supported bythe National Natural Science Foundation of China (NSFC, Grant No. 51905307), Chinese Postdoctoral Science Foundation (2019M662352), State Key Laboratory of Materials Processing and Die & Mould Technology, Huazhong University of Science and Technology (P2020-012), the National Natural Science Foundation of China (NSFC, Grant No. 51875318, 51905308), the Major Science and Technology Innovation Project of Shandong Province (Grant No. 2019JZZY020205) and the Qilu Outstanding Scholar Program of Shandong University.

References

1. B. Kim, W. Jang, J. Kim, C. W. Chung, Y. H. Park, and S. Choe, *Polym. Korea*, **25**, 855 (2001).
2. G. Wang, Y. Hui, L. Zhang, and G. Zhao, *Int. J. Heat Mass Transfer*, **116**, 1192 (2018).
3. M. Chen, D. G. Yao, and B. Kim, *Polym. Plast. Technol. Eng*., **40**, 491 (2001).
4. D. G. Yao and B. Kim, *Polym-Plast. Technol.*, **41**, 819 (2002).
5. G. Wang, G. Zhao, H. Li, and Y. Guan, *Mater. Des*., **31**, 3426 (2010).
6. G. Zhao, G. Wang, Y. Guan, and H. Li, *Polym. Adv. Technol.*, **22**, 476 (2011).
7. G. Wang, G. Zhao, H. Li, and Y. Guan, *Polym. Plast. Technol. Eng*., **48**, 671 (2009).
8. S. C. Chen, Y. C. Wang, S. C. Liu, and J. C. Cin, *Sens. Actuators A*, **151**, 87 (2009).
9. Z. Shayfull, S. Sharif, A. M. Zain, M. F. Ghazali, and R. M. Saad, *Adv. Polym. Technol*., **33**, 21381 (2014).
10. G. Wang, G. Zhao, and Y. Guan, *J. Appl. Polym. Sci*., **128**, 1339 (2013).
11. W. Wang, G. Zhao, Y. Guan, X. Wu, and Y. Hui, *J. Polym. Res.*, **22**, 84 (2015).
12. J. Vera, A. C. Brulez, E. Contraires, M. Larochette, N. Trannoy-Orban, M. Pignon, C. Mauclair, S. Valette, and S. Benayoun, *J. Micromech. Microeng*., **28**, 015004 (2018).
13. S. Meister, A. Seefried, and D. Drummer, *Microsyst. Technol*., **22**, 687 (2016).
14. X. Zhou, J. F. Feng, D. Cheng, J. J. Yi, and L. Wang, *Polymer*, **54**, 4719 (2013).
15. X. Zhou, J. C. Feng, J. J. Yi, and L. Wang, *Mater. Des.*, **49**, 502 (2013).
16. J. Q. Li, Z. Zhu, T. D. Li, X. Peng, S. F. Jiang, and L. S. Turng, *J. Appl. Polym. Sci*., **137**, 48581 (2020).
17. L. Crema, M. Sorgato, F. Zanini, S. Carmignato, and G. Lucchetta, *Compos. Part A-Appl. Sci. Manuf.*, **107**, 366 (2018).
18. M. Saniei, M. Tran, S. Bae, P. Boahom, P. Gong, and C. B. Park, *RSC Adv*., **109**, 108056 (2016).
19. J. L. Thomason, *Compos. Part A-Appl. Sci. Manuf.,* **33**, 1641 (2002).
20. A. Güllü, A. Özdemir, and E. Özdemir, *Mater. Des*., **27**, 316 (2006).
21. J. Q. Li, T. D. Li, Y. D. Jia, S. G. Yang, S. F. Jiang, and L. S. Turng, *Polym. Test*., **71**, 182 (2018).
22. P. Svoboda, C. C. Zeng, H. Wang, L. J. Lee, and D. L. Tomasko, *J. Appl. Polym. Sci.,* **85**, 1562 (2002).
23. A. Suplicz, F. Szabo, and J. G. Kovacs. *Thermochim Acta,* **574**, 145 (2013).
24. H. B. H. Salah, H. B. Daly, J. Denault, and F. Perrin, *Polym. Eng. Sci*., **53**, 905 (2013).
25. M. Fasihi, H. Garmabi, S. R. Ghaffarian, and M. Ohshima, *J. Appl. Polym. Sci*., **130**, 1834 (2013).
26. R. H. Olley and D. C. Bassett, *Polymer*, **23**, 1707 (1982).
27. A. Rozanski, A. Galeski, and M. Debowska, *Macromolecules*, **44**, 20 (2011).
28. G. Challa, P. H. Hermans, and A. Weidinger, *Makromolekulare Chemie*, **56**, 169 (1962).
29. ASTM D 638, "Standard Test Method for Tensile Properties of Plastics", 2003.
30. ASTM D790, "Standard Test Methods for Flexural Properties of Unreinforced and Reinforced Plastics and Electrical Insulating Materials", 2003.

31. J. Q. Li, H. C. Zhou, F. Y. Xu, S. F. Jiang, and W. Zheng, *Polym. Advan. Tchnol.*, **26**, 1312 (2015).
32. A. Romankiewicz, T. Sterzynski, and W. Brostow, *Polym. Int.*, **53**, 2086 (2004).
33. F. Jay, J. M. Haudin, and B. Monasse, *J. Mater. Sci.*, **34**, 2089 (1999).
34. G. Wang, G. Zhao, L. Zhang, Y. Mu, and C. B. Park, *Chem. Eng. J.*, **350**, 1 (2018).